Environmental Science & Technology

pubs.acs.org/est

Article

Nontarget Screening Exhibits a Seasonal Cycle of $PM_{2.5}$ Organic Aerosol Composition in Beijing

Jialiang Ma, Florian Ungeheuer, Feixue Zheng, Wei Du, Yonghong Wang, Jing Cai, Ying Zhou, Chao Yan, Yongchun Liu, Markku Kulmala, Kaspar R. Daellenbach,* and Alexander L. Vogel*

Cite This: *Environ. Sci. Technol.* 2022, 56, 7017−7028

Read Online

ACCESS | Metrics & More | Article Recommendations | Supporting Information

ABSTRACT: The molecular composition of atmospheric particulate matter (PM) in the urban environment is complex, and it remains a challenge to identify its sources and formation pathways. Here, we report the seasonal variation of the molecular composition of organic aerosols (OA), based on 172 $PM_{2.5}$ filter samples collected in Beijing, China, from February 2018 to March 2019. We applied a hierarchical cluster analysis (HCA) on a large nontarget-screening data set and found a strong seasonal difference in the OA chemical composition. Molecular fingerprints of the major compound clusters exhibit a unique molecular pattern in the Van Krevelen-space. We found that summer OA in Beijing features a higher degree of oxidation and a higher proportion of organosulfates (OSs) in comparison to OA during wintertime, which exhibits a high contribution from (nitro-)aromatic compounds. OSs appeared with a high intensity in summer-haze conditions, indicating the importance of anthropogenic enhancement of secondary OA in summer Beijing. Furthermore, we quantified the contribution of the four main compound clusters to total OA using surrogate standards. With this approach, we are able to explain a small fraction of the OA (~11−14%) monitored by the Time-of-Flight Aerosol Chemical Speciation Monitor (ToF-ACSM). However, we observe a strong correlation between the sum of the quantified clusters and OA measured by the ToF-ACSM, indicating that the identified clusters represent the major variability of OA seasonal cycles. This study highlights the potential of using nontarget screening in combination with HCA for gaining a better understanding of the molecular composition and the origin of OA in the urban environment.

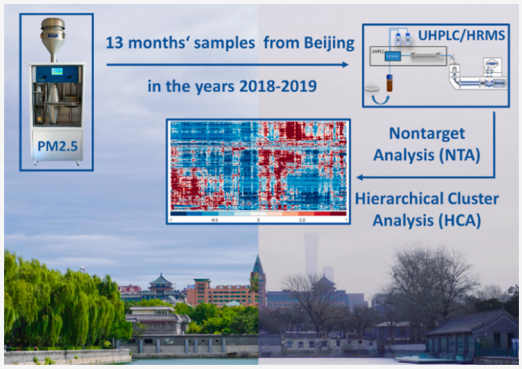

KEYWORDS: *particulate matter, urban aerosol, molecular composition, mass spectrometry, hierarchical cluster analysis*

1. INTRODUCTION

Atmospheric particulate matter (PM), in the form of liquid or solid particles suspended in air, can cause detrimental effects on human health depending on the particles chemical composition and their sources.[1,2] Furthermore, PM affects Earth's radiative balance through direct interaction with radiation and the formation of cloud condensation nuclei (CCN).[3] Organic aerosol (OA) represents a large proportion (20−90%) of the fine aerosol mass in the lower troposphere.[4−8] Thus, understanding the chemical composition and atmospheric transformation of OA is essential for understanding the sources and enables the identification of effective mitigation strategies. Among various aerosol components, OA typically represents ~30%−50% of the $PM_{2.5}$ mass concentration in China,[9,10] formed from a variety of natural and anthropogenic sources. Determining the chemical composition of urban OA at the molecular level is challenging due to the highly complex composition, represented by several thousands of compounds present at trace-level concentrations in a complex matrix. Therefore, the molecular-resolved characterization of OA requires the application of robust state-of-the-art analytical strategies.[11]

High-resolution mass spectrometry (HRMS) combined with electrospray ionization (ESI) has been widely applied to identify various organic compound classes.[12−14] The "soft" ESI technique, which converts the precursor molecules to molecular ions with minor fragmentation reactions, is advantageous for the determination of the molecular formulas of native organic compounds. High-resolution and accurate mass (HR/AM) measurement of the molecular ions and their isotopic patterns allow the determination of the molecular formulas of unknown compounds. Moreover, several studies have introduced the use of ESI-HRMS coupled with high-performance liquid chromatography (HPLC).[11,15−18] The separation of

Special Issue: Urban Air Pollution and Human Health

Received: October 13, 2021
Revised: March 9, 2022
Accepted: March 9, 2022
Published: March 18, 2022

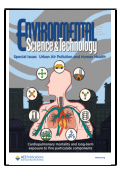

https://doi.org/10.1021/acs.est.1c06905
Environ. Sci. Technol. 2022, 56, 7017−7028

individual compounds by HPLC provides an additional dimension of information (e.g., on the polarity of the compounds), compared to HRMS studies using direct infusion. Furthermore, HPLC separation minimizes the variation arising from matrix ion suppression. For example, a previous study found a larger number of determined molecular formulas using HPLC combined with ESI-HRMS[19] than studies solely using direct infusion ESI-HRMS;[13,20−22] possibly caused by ion suppression reactions in the direct infusion technique. Moreover, separation by HPLC is a prerequisite for nontarget analysis (NTA) since algorithms use the information on retention time to attribute ions from fragmentation reactions, adduct and cluster formation reactions to their parent molecule.[23,24] However, care must be taken in setting up the individual NTA steps such as the detection and merging of features, filtering, and background correction.[25] In a recent NTA study of atmospheric PM preserved in an ice core, we demonstrated that applying different analysis software results in almost identical molecular fingerprints using HPLC-(−)ESI-HRMS.[26]

Haze episodes in Beijing attract worldwide attention and many studies using an HRMS approach have been conducted in Beijing.[19,27−32] For example, previous studies have revealed OA in winter Beijing is dominated by aromatics, which suggests a high contribution of combustion aerosols to the total OA.[19,27,33] Bryant et al.[29] discovered that the formation of isoprene-derived secondary organic aerosol (SOA) in urban Beijing is strongly influenced by anthropogenic emissions. Xie et al.[30] found that the number of detected compounds (especially for high molecular weight compounds) in aqueous PM extracts decreased with larger particle sizes. In this study, we applied NTA to HPLC-ESI-HRMS measurements of 172 ambient $PM_{2.5}$ filters from Beijing that cover a period of 13 months, and represent all detected compounds in comprehensive molecular fingerprints. Moreover, we used a hierarchical cluster analysis (HCA) for complexity reduction of the large data set that enabled the identification of compound classes that were likely to originate from similar sources and/or processes. Finally, we estimated the quantitative contribution of the four largest compound clusters to total OA based on calibrations using selected surrogate standards.

2. METHODS

2.1. Sampling, Filter Extraction, and Online Measurements. The ambient filters were collected at Beijing University of Chemical Technology (BUCT, 39°58′N,116°25′E), which is an urban site located in the North-East of Beijing.[34] 24 h integrated samples were collected during the period from 27 February 2018 to 30 March 2019 on preheated quartz-fiber filters (Ø150 mm, TISSUQUARTZ-2500QAT-UP, Pall Life Science, U.S.A.) by using a high-volume sampler (CAV-A/mb, MCV, Spain). We set the flow rate of the sampler to 30 m^3/h and collected samples every second or third day. In total, we collected 172 samples including 10 blank samples. Filter samples were sealed by aluminum foil and stored at −20 °C until analysis. For analysis, we punched 2 cm diameter circular sections from each filter and cut these sections into small pieces using ceramic scissors. Then we extracted the filters in an orbital shaker, twice for 20 min, consecutively, using 250 and 150 μL of an acetonitrile/water mixture (50/50 (v/v), acetonitrile: Optima LC/MS grade, Fisher scientific; water: 18.2 MΩ·cm, Millipak Express 40:0.22 μm, Millipore; Milli-Q Reference A+, Merck). After each extraction, we used a 0.22 μm polytetrafluoroethylene (PTFE) syringe filter (Fisher Scientific) and then combined the extracts in a sharp bottom vial (CS Chromatographie Service GmbH) for subsequent analysis.

At the same site, OA was simultaneously measured by a Time-of-Flight Aerosol Chemical Speciation Monitor (ToF-ACSM, details see Cai et al.[35] and Supporting Information, SI). Since the ToF-ACSM only measures nonrefractory $PM_{2.5}$ constituents, the $PM_{2.5}$ mass concentration used in this paper is the mean value of the Wanliu, Gucheng, Wanshouxigong, and Guanyuan monitoring stations, which are the nearest monitor sites operated by China National Environmental Monitoring Center (CNEMC). However, we note that the $PM_{2.5}$ mass concentrations measured by ToF-ACSM correlate well with the mean $PM_{2.5}$ values from these four monitoring stations (R = 0.89, SI Figure S1).

2.2. UHPLC-HRMS Analysis. The analysis of the filter extracts was conducted with an Orbitrap HRMS (Q Exactive Focus Hybrid-Quadrupol-Orbitrap, Thermo Scientific) coupled with an ultrahigh performance liquid chromatography (UHPLC) system (Vanquish Flex, Thermo Fisher Scientific). The chromatographic separation was performed on a reversed phase column (Accucore C_{18}, 150 × 2.1 mm, 2.6 μm particle size, Thermo Scientific), at 40 °C (still air). As mobile phases we used eluent A (ultrapure water with 0.1% formic acid (LiChropur, Merck), v/v) and eluent B (acetonitrile with 0.1% formic acid, v/v). The gradient was set as follows: starting with 1% B for 2.0 min, increased to 99% B within 13 min, held for 2 min, decreased to 1% B within 1 min and finally held for 2 min for re-equilibration. The flow rate was 0.4 mL/min, and the injection volume was 2 μL. It is worth mentioning that due to the large set of samples, the UHPLC-HRMS measured continuously for 6 days to complete the measurements. Consequently, we repeated the measurement of one sample on a daily basis to monitor the performance of the instrument. We observe a highly reproducible instrumental performance in terms of intensity variation and mass accuracy of the five quantified compounds (4-Nitrophenol, 4-Nitrocatechol, Phthalic acid, 3-methyl-1,2,3-butanetricarboxylic acid (MBTCA), and Pinic acid) during the measurement period (see Figures S2 and S3). The mass spectra (m/z 50−750) with a resolving power of 70 000@ m/z 200 were obtained by using (−)ESI. Ion source settings were as follows: 8 psi auxiliary gas (nitrogen), 40 psi sheath gas (nitrogen), 3.5 kV spray voltage, and 350 °C gas temperature.

2.3. UHPLC-HRMS Data Processing. We used the NTA software (Compound Discoverer (CD), version 3.2, Thermo Fisher Scientific) to identify chromatographic peak features in the two-dimensional space of retention time and m/z. These features are combined to compounds when eluting at the same retention time and appearing at a m/z that corresponds to the exact mass differences from either isotopes, adducts, clusters or fragments. On the basis of the HR/AM-measurement and the isotopic pattern, molecular formulas for the detected compounds were calculated. The detailed settings of the CD-workflow are provided in Table S1.

A brief description of the NTA-workflow: a threshold intensity of 1E6 was applied to the two-dimensional coordinate system (RT: 0−20 min, m/z: 50−750) for all 172 measurements. CD automatically filtered out ions with peak abundance below the threshold intensity, as well as the ions that appeared in blank samples at intensities of >1/3 of the maximum values of the ambient samples. For the remaining ions, the molecular

https://doi.org/10.1021/acs.est.1c06905
Environ. Sci. Technol. 2022, 56, 7017−7028

formulas were calculated with elemental combinations of $C_{n1}H_{n2}Br_{n3}Cl_{n4}N_{n5}O_{n6}P_{n7}S_{n8}$ (n1 = 1−90, n2 = 1−190, n3 = 0−3, n4 = 0−4, n5 = 0−4, n6 = 0−20, n7 = 0−1, and n8 = 0−3) and with a mass tolerance of 2 ppm. To filter out chemically unreasonable formulas, the minimum H/C and maximum H/C were set as 0.1 and 3.5, respectively.

2.4. Calculation of Molecular Characteristics. The double bond equivalent (DBE) of a molecular formula containing C, H, N, O, and S indicates the number of rings, double and triple bonds. The value of the DBE is calculated based on the number of the individual elements as follows:[36]

$$\mathrm{DBE} = \#\mathrm{C} - \frac{\#\mathrm{H}}{2} + \frac{\#\mathrm{N}}{2} + 1 \quad (1)$$

Both the aromaticity equivalent[37] (Xc) and aromaticity index[38] (AI) can be applied to estimate the aromaticity of the organic compounds. Here we used Xc as it classifies (poly)aromatic compounds with significant alkylation as aromatic compounds.[39] Thus, Xc was applied in this study to estimate the aromaticity of the compounds, expressed as follows:

$$\mathrm{Xc} = \frac{3*[\mathrm{DBE} - (m*\#\mathrm{O} + n*\#\mathrm{S})] - 2}{\mathrm{DBE} - (m*\#\mathrm{O} + n*\#\mathrm{S})} (0 \text{ if } < 0) \quad (2)$$

Here "m" and "n" are the fractions of oxygen and sulfur atoms in the π-bond structures of a compound (both "m" and "n" are presumed to be 0.5[37]), respectively. If the DBE $\leq m*\#O + n*\#S$, then Xc = 0, showing no aromaticity as Yassine et al.[37] suggested that compounds with Xc < 2.5000 correspond to nonaromatic compounds, for aromatics 2.5000 $\leq$ Xc < 2.7143 and for condensed aromatics Xc $\geq$ 2.7143.

All the observed formulas were classified into six categories based on their elemental compositions, including CHOa, CHOn, CHNO, CHNOS, CHOS, and others. As an example, CHOS refers to compounds that contain the elements carbon, hydrogen, oxygen, and sulfur. The compound categories CHOa represent aromatics (Xc $\geq$ 2.5), while CHOn are nonaromatic (Xc < 2.5) compounds (e.g., terpene oxidation products). "Others" (e.g., CH, CHS, CHNS, and signals to which no elemental formulas were calculated) refers to the compounds excluded from the above major compound categories.

2.5. Hierarchical Cluster Analysis. HCA is a data mining method that merges individual observations into clusters of similar behavior through the determination of the similarity between every pair of objects in a data matrix. Previous studies have described the principle of HCA in detail[40,41] and discuss its difference to other methods, such as the widely used positive matrix factorization (PMF). In brief, HCA groups compounds in a stepwise process in contrast to PMF that defines components (termed factors) that explain the compounds' variability. In this work, we use Matlab (Mathworks) to perform the HCA. The observation used as input for the HCA was a matrix of organic compounds and their peak area in the 172 samples covering a time span of 13 months. As a first step, the peak areas were standardized based on z-transformation. The proximity between the observation pairs was determined by Euclidean distance for both compound rows and sample columns. We note that it is also possible to use other metrics of distance, for example, correlation or cosine distance, however, the Euclidean distance made our data set the most understandable and reproducible. We used the Ward linkage method for merging different compounds and samples into compound clusters and sample clusters, respectively. The hierarchical clustering in this study was performed twice, on both compound rows and sample columns. Moreover, the two clusterings were independent from each other since the order of components does not matter when one computes the distance between two vectors.

The outcome of the NTA resulted in 2136 compounds after background correction, filtering for duplicates, and applying an intensity threshold for the sample-to-blank ratio of >3. In order to avoid a bias in the HCA introduced by a large number of small signals, we used, as input, only the major compounds that were responsible for 94% of the total peak area (SI Figure S4). Variation of this threshold does not affect the compound clustering. However, with 95% as input we observe a slight difference of the sample clustering, but with 94% as input we observe a better separation between summer samples into clean and haze conditions. With using 94% as input, there were 1323 compounds remaining, of which 1097 had unambiguous molecular formulas.

3. RESULTS AND DISCUSSION

3.1. Seasonal Differences of the OA Chemical Composition in Beijing. Figure 1 indicates a clear seasonal variation in the intensities and the relative contribution of different compound categories (Figure 1A and B). We observed an enhanced absolute intensity of organic compounds (Figure 1C), especially for the intensity of the compound groups CHNO (e.g., nitroaromatics) and CHOa (e.g., oxidized aromatics), which contribute 38% and 17%, respectively, to the total peak intensity during winter. These specific compound groups are likely attributed to the increased solid fuel combustion activities in winter.[33] Moreover,

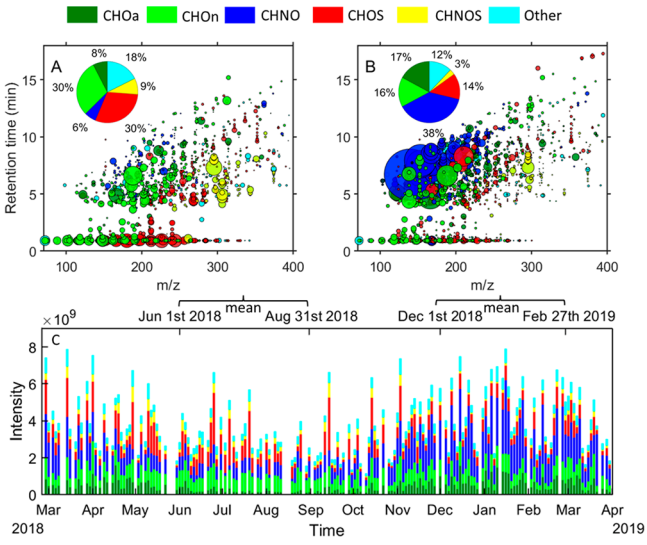

Figure 1. Seasonal differences and time series for the intensity of OA chemical composition. (A, B) The m/z vs retention time (RT) plots represent a three-month mean value of summer (A) and winter (B) samples. Individual detected compounds are displayed as circles with the area representing the signal intensity, and the color indicates the molecular composition. The x-axes show the mass-to-charge ratio (m/z) of the compounds, and the measured retention time (y-axis) indicates the polarity of the single molecules. (C) Time series of the different compound categories (CHOn, CHOa, CHNO, CHOS, CHNOS, and others).

https://doi.org/10.1021/acs.est.1c06905
Environ. Sci. Technol. 2022, 56, 7017−7028

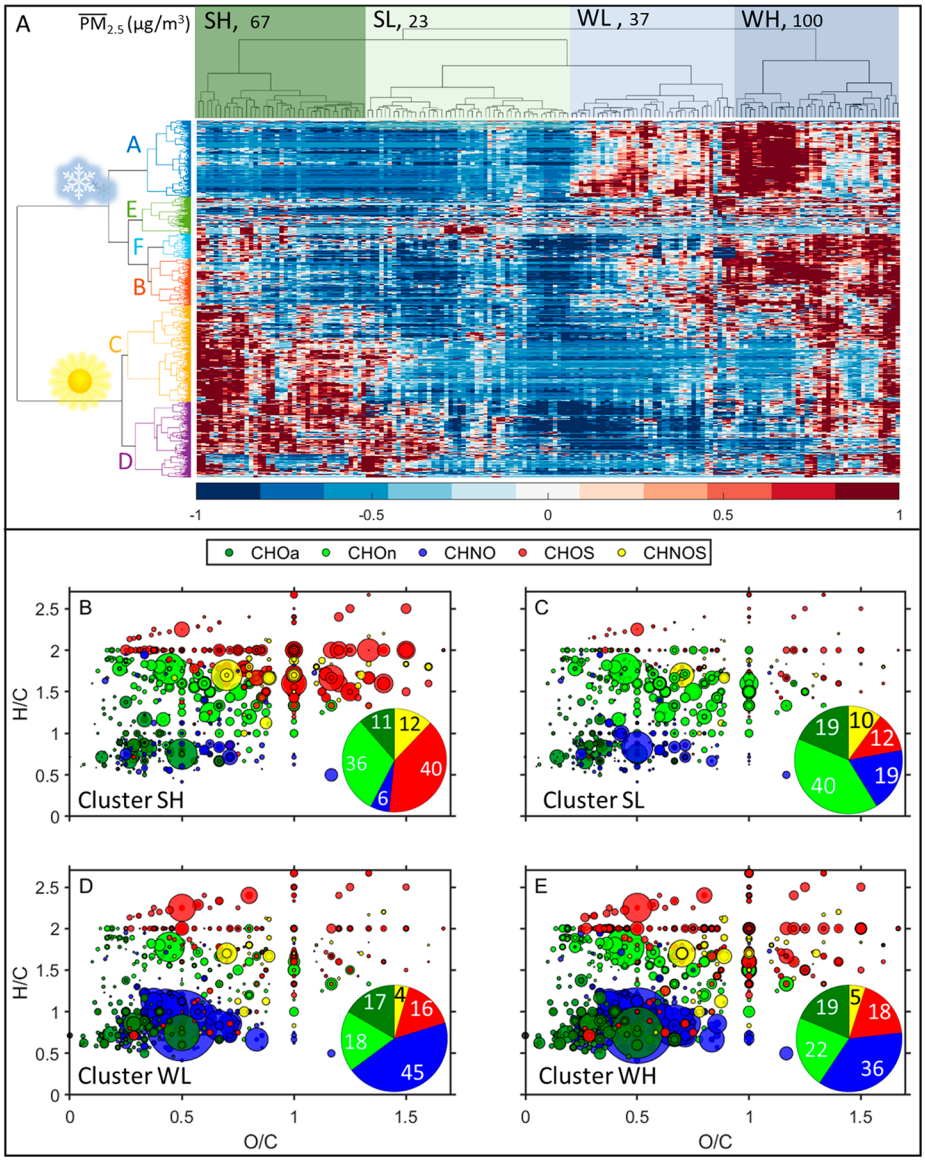

Figure 2. HCA and molecular fingerprints. (A) Hierarchical clustergram: the *x*-axis and *y*-axis represent the sample cluster and compound cluster, respectively. The letters A–F in the *y*-axis represent the respective compound clusters. Sun: compound clusters high in summer, snowflake: compound clusters high in winter. (B–E) show the average intensities for samples from the summer high PM (SH), summer low PM (SL), winter low PM (WL), and winter high PM (WH) days, respectively, in a Van Krevelen-diagram. The numbers inside the pie chart represent the intensity contribution (%) of each compound category to the total detected compound intensity.

unfavorable meteorological conditions (e.g., low wind speed, stagnation of air, and a shallow and stable inversion layer) may promote OA accumulation in Beijing during winter.[42] In contrast, the relative contribution of these two groups to the total intensity in summer are 6% and 8%, respectively. The major compounds in these two groups have an RT > 4.5 min, indicating their relatively low polarity. Contrary to the enhancement of the CHNO and CHOa compounds, the CHOn, CHOS, and CHNOS compounds show decreased abundance in winter, accounting for 16%, 14%, and 3% of the total intensity, respectively. The relative contribution of the CHOn compounds to the total intensity in summer is 30%, which can partly be explained by enhanced biogenic emissions in summer. On the basis of MS^2–spectra and retention time, we are able to unambiguously identify CHOn compounds as oxidation products of certain biogenic VOCs.[26] Moreover, low temperatures during winter may lead to lower evaporation of anthropogenic CHOn compounds. A clear decrease of CHOn with short retention times was observed for the winter season, similar to the trend for CHOS compounds (e.g., isoprene-organosulfates (OSs)), which contribute up to 30% of the total intensity in summer. The CHOS compounds display a wide spectrum in polarity, ranging from polar (short RT) to nonpolar (long RT) compounds. Due to more oxygen- and heteroatoms, the CHNOS compounds tend to have higher mass-to-charge ratios (m/z) than most of the other compounds. The relative contribution of CHNOS compounds in summer is 9%. The formation of OSs can enhance PM mass, since the sulfate-functionalization of small organic compounds (e.g., from isoprene oxidation) changes the gas-to-particle partitioning of these small organic molecules toward the particle phase. Furthermore, some of the OSs are hygroscopic and light-absorbing,[43−45] hence this class of compounds may enhance haze in summer. However, further research on the

https://doi.org/10.1021/acs.est.1c06905
Environ. Sci. Technol. 2022, 56, 7017−7028

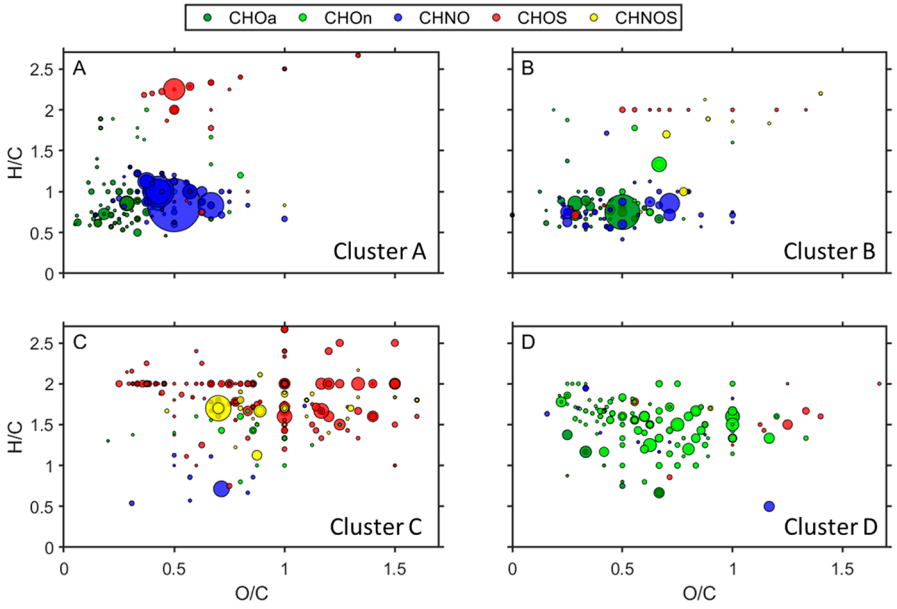

Figure 3. Comparison of compounds that originate from different sources, illustrated in the Van Krevelen space (peak area shows the mean intensity of all 172 samples). (A–D) Van Krevelen diagram of clusters A–D from HCA (see Figure 2).

quantification of the organosulfate effect on urban haze is needed. Finally, we like to emphasize that the peak intensities in Figure 1 are not directly linked to the concentration of the individual compounds, however, differences of peak intensities of the same compound (category) throughout the time series can be interpreted.

3.2. Application of Hierarchical Cluster Analysis on 172 PM Samples. We used the filtered data matrix to (1) display molecular fingerprints of the average intensity (Figure S5A,B), (2) perform a HCA (Figure 2A), and (3) identify groups of samples (Figure 2B–E) and compounds that exhibit similar temporal patterns (Figure 3A–D).

The horizontal and vertical dendrograms in Figure 2A visualize the distance between different samples and different compounds, respectively. Interestingly, we found that the horizontal dendrogram clearly separated the samples into summer high PM (SH, haze episodes), summer low PM (SL), winter low PM (WL), and winter high PM (WH, haze episodes) clusters by comparison with $PM_{2.5}$ mass concentration (Figure 2A). The mean $PM_{2.5}$ mass of clusters SH, SL, WL, and WH was 67 $\mu g/m^3$, 23 $\mu g/m^3$, 37 $\mu g/m^3$, and 100 $\mu g/m^3$, respectively (the distribution of $PM_{2.5}$ mass of these four clusters is shown in Figure S6). We observed a strong variation of the organic aerosol composition by plotting the molecular fingerprints of clusters SH, SL, WL, and WH (average intensity, Figure 2B–E). Most clearly, the majority aliphatic OSs, which appeared in the SH samples, are not detected in the SL samples. The relative contribution of the CHOS compounds to the total intensity in cluster SH is 40%, which is much higher than in cluster SL (12%, Figure 2B and C). This observation indicates that the formation of aliphatic OSs (at high particulate sulfate concentration and high relative humidity[46]) can be an important factor for the increase of organic aerosol mass in summer Beijing. The organic aerosol composition was similar in the clusters WL and WH, however, the compound intensity of cluster WH was much higher than that of cluster WL. This may indicate that the emission sources and chemical processes in winter are relatively constant, and OA pollution accumulates when wind speed is low. In fact, we observe that both low-pollution episodes experienced higher wind speed, and the backward trajectories show that the air masses were coming from the northwest to north sector (see Figure S7A,B).

Regarding the clustering result of the compounds (vertical dendrogram), we observed two separate clusters: the compounds in the upper cluster were abundant in winter, while the lower cluster's compounds had a higher intensity in summer. In order to elucidate this seasonal variation in the chemical properties of the compounds (e.g., molecular formula, oxidation state, aromaticity), we divided them into smaller clusters. The Van Krevelen diagrams in Figure 3 display the compound clusters A–D. It becomes evident that the HCA is a powerful tool that reduces the chemical complexity by aggregating compounds of similar chemical characteristics into the same clusters (clusters A, B, C, and D, Figure 3). Clusters E and F either have no clear chemical patterns in the Van Krevelen-space (Figure S8A) or contain very small amounts of aliphatic compounds (Figure S8B), therefore, these two clusters will not be discussed further.

Figure 3A shows that this cluster is dominated by the CHNO compounds, followed by the CHOa compounds. The majority of the compounds appear at the region of $0.2 < H/C < 1.2$ and $0.3 < O/C < 0.6$, indicating that CHNO and CHO aromatics are important compound classes in wintertime Beijing. We found the homologous series of $C_{5+n}H_{3+2n}NO_3$ (n = 1–5) and $C_{5+n}H_{3+2n}NO_4$ (n = 1–4) in this cluster with slopes of −2.33 and −1.75, respectively (y-intercept at H/C = 2). The largest signals of the two series corresponded to $C_6H_5NO_3$ and $C_6H_5NO_4$, which were identified (by comparing the retention time and fragmentation pattern with the authentic standards, Figure S9A,B) as 4-nitrophenol and 4-nitrocatechol, respectively. Previous studies have identified nitroaromatics as oxidation products of coal burning,[47,48] biomass burning,[49−51] and vehicle emissions.[52−55] A recent study by Yuan et al. suggests that coal and biomass burning in winter are the major sources for nitroaromatics.[56] Furthermore, previous studies have also revealed that in winter, nitrophenol and nitrocatechol are likely arising from biomass

https://doi.org/10.1021/acs.est.1c06905
Environ. Sci. Technol. 2022, 56, 7017−7028

and coal burning emissions.[55,57,58] In addition, we observed $C_7H_6O_3$ as a major compound in this cluster, being tentatively identified as monohydroxy benzoic acid, which is a tracer compound for naphthalene oxidation.[59,60]

In cluster B, CHOa compounds were the most abundant compounds (according to the intensities of the compounds), followed by CHNO compounds (Figure 3B). Most of the compounds appear in the area of 0.5 < H/C < 1.2 and 0.25 < O/C < 0.8, which indicates an aromatic character. The largest signal of this cluster was identified as phthalic acid ($C_8H_6O_4$, Figure S9C), which is a product of naphthalene photooxidation.[61,62] Similarly, phthalic acid has also been reported as a product of vehicle exhaust and biomass burning.[39,60,63,64] We observed that the most abundant compounds in this cluster have a carbon number between 6 and 10 (Figure S10A). In this range, these compounds could be associated with the oxidation products of benzene, toluene, ethylbenzene, xylene (BTEX), C3- and C4-benzenes, all of which were previously observed in emissions from traffic and coal burning in north China.[65−69] Simultaneously, the homologous series of aliphatic organosulfates in both clusters A and B are tentatively classified as alkylorganosulfates (cluster A: $C_nH_{2n+2}SO_4$, n = 3−11, cluster B: $C_nH_{2n}SO_5$, n = 7−10), which are described as markers for secondary traffic OA.[14] As consequence, we infer that the compounds in clusters A and B originate mainly from solid fuel combustion and traffic emissions.

As Figure 3C indicates, almost all compounds in cluster C are sulfur-containing compounds (CHOS and CHNOS). Interestingly, most of the sulfur-containing compounds fall into the area of 1.5 < H/C < 2 and 0.3 < O/C < 1.5. The high H/C ratio indicates that the S-containing compounds are affected by more aliphatic precursors, while the high O/C ratio suggests that they also have a high oxidation state. As previous studies indicate, the CHOS compounds which fulfill O/S ≥ 4 can be tentatively classified as OSs.[19,31,60,70] Thus, a large majority (>99%) of CHOS compounds in this cluster could be assigned as OSs (by peak intensity). We also found the homologues of $C_nH_{2n}SO_5$ (n = 4−17) and $C_nH_{2n}SO_6$ (n = 4−16) appearing in the diagram at H/C = 2; such aliphatic OSs were reported as products from the reaction of SO_2 with emissions from liquid fossil fuel.[12,26,60] However, there are also plenty of very polar OSs with extremely short retention times (Figure S5A); most of these have less than 10 carbon atoms (Figure S10B). In this range, one can expect OSs from biogenic emissions; for example, we find $C_5H_8SO_7$ that has been reported as an isoprene-derived organosulfate,[71,72] while $C_6H_{10}SO_6$ and $C_6H_{10}SO_7$ have been reported as OSs formed from the OH-initiated oxidation from green leaf volatiles.[73] Furthermore, six isomers of the monoterpene-derived nitrooxy-OS ($C_{10}H_{17}NO_7S$),[46,74] were also observed in this cluster. These compounds have relatively high intensities during summertime, when biogenic emissions are high and radiation can accelerate the formation of sulfate and OSs from SO_2 emissions.[74−76] Overall, this organosulfate cluster has diverse sources with clear contributions from liquid fossil fuel and biogenic emissions.

The majority of compounds in Cluster D (Figure 3D) are CHOn compounds, present in the region of 1.1 < H/C < 2 and 0.2 < O/C < 0.9. Previous studies suggest that in this region oxidation products of biogenic emissions appear.[26,39,77] We confirm this cluster as partly biogenic as we detect the compounds MBTCA ($C_8H_{12}O_6$) and pinic acid ($C_9H_{14}O_4$), which are widely used as oxidation tracers of α-pinene (Figure S9D,E).[78−81] However, we cannot exclude the contribution of anthropogenic compounds in this cluster. For instance, the CHO compounds with 11 and 12 carbons and $\overline{OS}_C$ between −1 and 0 appear with a high signal in this cluster (Figure S10C). These compounds are likely oxidation products of anthropogenic emissions since the oxidation of terpenes rarely results in C_{11}- and C_{12}-compounds.[82]

3.3. Concentration Time Series of the Compounds in the Different Clusters and Their Relative Contribution to the Total OA. In atmospheric sciences, the use of surrogates to quantify similar compounds is a common approach when authentic standards are not available.[11] However, for NTA, it is impossible to allocate authentic or surrogate standards for every compound. Hence, it is a challenge to quantify nontarget screening data. Here, we used the average response of different surrogate standards to quantify the sum of the signal intensities of the four main compound clusters A−D.

We calibrated the system with eight different standards (Figure S11) and found that 4-nitrophenol and 4-nitrocatechol had the highest responses of the eight surrogates. This indicated that nitroaromatics have a higher ionization efficiency in (−)ESI than other compounds, hence, we used the average response of these two standards to quantify the nitroaromatic compounds present in clusters A and B. However, the ionization efficiency for different CHOa compounds varied greatly and, in order to minimize deviation, we tested three CHOa compounds (5,7-dihydroxy-4- phenylcoumarin, phthalic acid, and benzoic acid) and took the average of their responses to quantify the CHOa compounds in clusters A and B (Figure S11). Furthermore, camphor-10-sulfonic acid has been widely suggested to be used as the surrogate standard to quantify OSs,[83−85] therefore, this was employed to quantify OSs in cluster C in our study. The calibration curves of MBTCA and pinic acid are very similar (Figure S11). Therefore, we used the mean response of MBTCA and pinic acid to quantify compounds in cluster D. Certainly, this approach of quantification for this large data set can easily introduce an error of a factor of 2. However, in this analysis, we observe that the Pearson correlation coefficients between the four clusters A−D and OA mass (determined by ToF-ACSM; A-OA: 0.44, B-OA: 0.70, C-OA: 0.51, and D-OA: 0.41 (Figure 4)) are all lower than the correlation coefficient between the sum of the four clusters and the OA mass (R = 0.78). This indicates that the used quantification method does not introduce any bias by giving more weight to one of the clusters, but instead explains the rather flat OA observation by the different seasonal contribution of the identified clusters (Figure 4). Furthermore, the concentration of OSs in cluster C are in the same range with other recent studies that determined the content of organic sulfates in Beijing.[29,86]

The time series in Figure 4 reveal a strong seasonal variation of the concentration of the four different clusters. The aromatic compounds in clusters A and B show a clear increasing trend during the domestic-heating period, which provides further evidence for the OA from solid fuel combustion and traffic emissions. The lower appearance of aliphatic organosulfur-compounds (as traffic markers) in summer can be explained by a faster chemical degradation due to OH radicals, and more efficient mixing in a higher boundary layer. Cluster B shows a higher fluctuation during winter than cluster A, which might be explained as a combined meteorological and photochemical effect. In contrast, the compounds in clusters C and D are

https://doi.org/10.1021/acs.est.1c06905
Environ. Sci. Technol. 2022, 56, 7017−7028

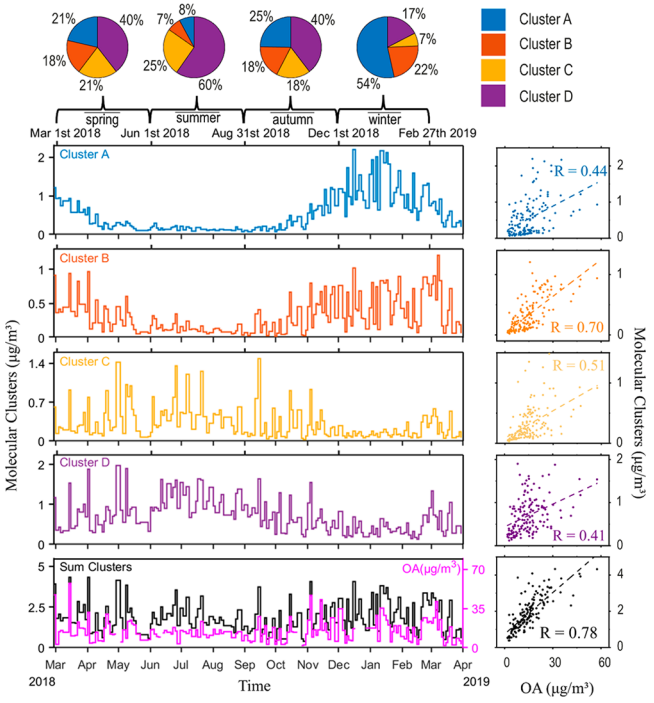

Figure 4. Concentration time series of compounds in clusters A, B, C, D, sum of the four clusters, and OA (data from ACSM). The scatter plots show the correlation between the four individual cluster and OA, as well as the correlation between the sum of the four clusters and the OA content. The pie charts display the concentration fractions of individual cluster in sum of the four clusters in spring, summer, autumn, and winter.

more abundant in summer, which indicates that these compounds partly originate from biogenic emissions. The strong positive correlation (R = 0.75, Figure S12) between these two clusters suggest that some of these compounds have the same source. Compounds from cluster C are elevated with increasing sulfate mass concentrations (Figure S12), which indicates the importance of sulfate in the secondary formation of OSs.[31] The concentration of these compounds in the two clusters greatly fluctuates from day to day, and thus reveal that these clusters are largely dependent on meteorological conditions (air mass origin, relative humidity, temperature, radiation, wind speed, and so forth). It is worth mentioning that the compounds in cluster D also have a relatively high content in winter (ranging from 120 to 920 ng/m^3, with a mean of 380 ng/m^3); this provides further evidence that a part of the compounds from this cluster are also influenced by anthropogenic activities. Interestingly, although the concentration time series of the compounds in every individual cluster shows a clear seasonal cycle, the time series for the sum concentration of the four clusters does not exhibit a seasonal variation; this is in agreement with the time series of OA from the ACSM measurement (Figure 4). Thus, there is a strong correlation between the sum of the quantified clusters and OA, indicating that the cluster analysis represents the major variability of OA seasonal cycles.

In order to investigate further the concentration fraction of the four clusters in relation to the total OA, we averaged the concentration of the sum clusters in spring, summer, autumn, and winter, respectively, the same was applied to the total OA content. As the pie charts in Figure S13 indicate, with this approach we can explain only a small fraction of OA (~11–14%). However, in the nontarget data set we found sufficient evidence for seasonal variation; for example, clusters A and B represent emissions of solid fuel combustion and traffic, contributing with 76% to the total of the four main clusters in winter, but only 15% in summer. The CHOn cluster (cluster D) showed a relative contribution of 60% in summer and only 17% in winter (see Figure 4). To gain a more complete insight on ambient OA and its sources, other ionization approaches need to be applied to enable the detection of the remaining unattributed OA.

3.4. Limitations and Implications. As limitations we emphasize that the UHPLC/HRMS technique only identifies a small fraction of the total OA, and also potential sampling artifacts cannot be ignored (e.g., α-pinene oxidation products can react with SO_2 during filter sampling[87]). The six compound categories do not represent the entire organic composition since electrospray ionization is not sensitive to nonpolar compounds (e.g., nonfunctionalized polycyclic aromatic hydrocarbons, hopanes, and alkanes).[13] Furthermore, (−)ESI is also not sensitive to compounds with no acidic protons (e.g., phthalates). To a lesser extent, there might be large-molecular weight humic-like substances (HULIS), that we do not detect in the scanning mass range of the mass spectrometer, or which do not result in sharp chromatographic peaks.[88]

Nevertheless, the nontarget screening in combination with HCA can help to gain a more comprehensive understanding of urban air pollution at the molecular level. With this approach, we were able to distinguish high PM and low PM samples from different seasons and to determine the variation of the organic aerosol composition. Moreover, we can infer the different sources of the organic compounds from the chemical composition patterns and observe enhanced organosulfate formation during summer haze episodes. Further studies are needed to confirm attribution of OA winter clusters to anthropogenic emissions from coal combustion, biomass burning and traffic as well as quantitatively identify the major primary OA (POA) and SOA sources.

The calibration method in our study bridges the gap to quantify compounds from ESI-NTA. The strong correlation between the sum of the quantified clusters and OA indicates that the cluster analysis represents the major variability of OA seasonal cycles. We suggest that future nontarget studies of OA could follow the direction of combining different ionization techniques to provide a more comprehensive data set for NTA of ambient filters. Joint effort is needed to establish a mass spectrometry database that contains molecular fingerprints of chamber-generated organic aerosol, in order to identify sources and their contribution to OA in ambient samples.

■ ASSOCIATED CONTENT

Supporting Information

The Supporting Information is available free of charge at https://pubs.acs.org/doi/10.1021/acs.est.1c06905.

Detailed information on the ACSM measurement; CD-workflow settings and identified molecules; additional information on the $PM_{2.5}$ correlation between monitoring sites and ACSM; QA/QC of UHPLC/HRMS measurements; data preparation for HCA; molecular fingerprints (average intensity); histogram of $PM_{2.5}$ mass of clusters SH, SL, WL, and WH; backward trajectory and wind rose of the sampling period; Van Krevelen-

https://doi.org/10.1021/acs.est.1c06905
Environ. Sci. Technol. 2022, 56, 7017−7028

diagram of clusters E and F; MS/MS fragmentation spectra of quantified compounds; Kroll-diagram of clusters B, C, and D; calibration curves; relationship between clusters C and D and sulfate; and fraction of the four clusters to the total OA (PDF)

AUTHOR INFORMATION

Corresponding Authors

Kaspar R. Daellenbach − *Aerosol and Haze Laboratory, Beijing Advanced Innovation Center for Soft Matter Science and Engineering, Beijing University of Chemical Technology, 100029 Beijing, P. R. China; Institute for Atmospheric and Earth System Research/Physics, Faculty of Science, University of Helsinki, 00014 Helsinki, Finland; Laboratory of Atmospheric Chemistry, Paul Scherrer Institute, 5232 Villigen, Switzerland*; Email: kaspar.daellenbach@psi.ch

Alexander L. Vogel − *Institute for Atmospheric and Environmental Sciences, Goethe-University Frankfurt, 60438 Frankfurt am Main, Germany;* orcid.org/0000-0002-1293-6370; Email: vogel@iau.uni-frankfurt.de

Authors

Jialiang Ma − *Institute for Atmospheric and Environmental Sciences, Goethe-University Frankfurt, 60438 Frankfurt am Main, Germany;* orcid.org/0000-0003-0815-4066

Florian Ungeheuer − *Institute for Atmospheric and Environmental Sciences, Goethe-University Frankfurt, 60438 Frankfurt am Main, Germany;* orcid.org/0000-0002-4557-3844

Feixue Zheng − *Aerosol and Haze Laboratory, Beijing Advanced Innovation Center for Soft Matter Science and Engineering, Beijing University of Chemical Technology, 100029 Beijing, P. R. China*

Wei Du − *Aerosol and Haze Laboratory, Beijing Advanced Innovation Center for Soft Matter Science and Engineering, Beijing University of Chemical Technology, 100029 Beijing, P. R. China; Institute for Atmospheric and Earth System Research/Physics, Faculty of Science, University of Helsinki, 00014 Helsinki, Finland*

Yonghong Wang − *Aerosol and Haze Laboratory, Beijing Advanced Innovation Center for Soft Matter Science and Engineering, Beijing University of Chemical Technology, 100029 Beijing, P. R. China; Institute for Atmospheric and Earth System Research/Physics, Faculty of Science, University of Helsinki, 00014 Helsinki, Finland; Research Center for Eco-Environmental Sciences, Chinese Academy of Sciences, 100085 Beijing, P. R. China;* orcid.org/0000-0003-2498-9143

Jing Cai − *Aerosol and Haze Laboratory, Beijing Advanced Innovation Center for Soft Matter Science and Engineering, Beijing University of Chemical Technology, 100029 Beijing, P. R. China; Institute for Atmospheric and Earth System Research/Physics, Faculty of Science, University of Helsinki, 00014 Helsinki, Finland*

Ying Zhou − *Aerosol and Haze Laboratory, Beijing Advanced Innovation Center for Soft Matter Science and Engineering, Beijing University of Chemical Technology, 100029 Beijing, P. R. China*

Chao Yan − *Aerosol and Haze Laboratory, Beijing Advanced Innovation Center for Soft Matter Science and Engineering, Beijing University of Chemical Technology, 100029 Beijing, P. R. China; Institute for Atmospheric and Earth System Research/Physics, Faculty of Science, University of Helsinki, 00014 Helsinki, Finland*

Yongchun Liu − *Aerosol and Haze Laboratory, Beijing Advanced Innovation Center for Soft Matter Science and Engineering, Beijing University of Chemical Technology, 100029 Beijing, P. R. China;* orcid.org/0000-0002-9055-970X

Markku Kulmala − *Aerosol and Haze Laboratory, Beijing Advanced Innovation Center for Soft Matter Science and Engineering, Beijing University of Chemical Technology, 100029 Beijing, P. R. China; Institute for Atmospheric and Earth System Research/Physics, Faculty of Science, University of Helsinki, 00014 Helsinki, Finland*

Complete contact information is available at: https://pubs.acs.org/10.1021/acs.est.1c06905

Author Contributions

J.M. did the majority of data curation and analysis, and wrote the original manuscript. J.M. and F.U. performed the UHPLC/HRMS measurements and nontarget analysis. F.U. synthesized standards. F.Z., W.D., Y.W., J.C., Y.Z., C.Y., and Y.L. collected the ambient filters and performed the ACSM measurement. K.R.D., M.K., and A.L.V. managed the project, advised on data analysis, edited and revised the manuscript. All authors have contributed to the scientific discussion and have given approval to the final version of the manuscript.

Notes

The authors declare no competing financial interest.

Data availability. The data underlying this study are openly available in zenodo.org at DOI: 10.5281/zenodo.6354745.

ACKNOWLEDGMENTS

J.M. thanks the China Scholarship Council (CSC) for the life expense covering (NO.202008080054). K.R.D. acknowledges support by the SNF mobility grant P2EZP2_181599. M.K. acknowledges the following projects: ACCC Flagship funded by the Academy of Finland grant number 337549, Academy professorship funded by the Academy of Finland (grant no. 302958), Academy of Finland projects no. 1325656, 316114, and 325647, "Quantifying carbon sink, CarbonSink+, and their interaction with air quality" INAR project funded by Jane and Aatos Erkko Foundation, European Research Council (ERC) project ATM-GTP Contract No. 742206. This research has been supported by the Deutsche Forschungsgemeinschaft (DFG; German Research Foundation) (grant no. 410009325).

ABBREVIATIONS

AI, aromaticity index; BUCT, Beijing University of Chemical Technology; CCN, cloud condensation nuclei; CD, Compound Discoverer; CNEMC, China National Environmental Monitoring Center; DBE, double bond equivalent; ESI, electrospray ionization; HCA, hierarchical cluster analysis; (U)HPLC, (ultra)high performance liquid chromatography; HR/AM, high-resolution and accurate mass; HRMS, High-resolution mass spectrometry; MBTCA, 3-methyl-1,2,3-butanetricarboxylic acid; NTA, nontarget analysis; OA, organic aerosols; OSs, organosulfates; PM, particulate matter; PMF, positive matrix factorization; POA, primary organic aerosol; PTFE, polytetrafluoroethylene; SOA, secondary organic aerosol; ToF-ACSM, Time-of-Flight aerosol chemical speciation monitor; Xc, aromaticity equivalent

https://doi.org/10.1021/acs.est.1c06905
Environ. Sci. Technol. 2022, 56, 7017−7028

REFERENCES

(1) Daellenbach, K. R.; Uzu, G.; Jiang, J.; Cassagnes, L.-E.; Leni, Z.; Vlachou, A.; Stefenelli, G.; Canonaco, F.; Weber, S.; Segers, A.; Kuenen, J. J. P.; Schaap, M.; Favez, O.; Albinet, A.; Aksoyoglu, S.; Dommen, J.; Baltensperger, U.; Geiser, M.; El Haddad, I.; Jaffrezo, J.-L.; Prévôt, A. S. H. Sources of Particulate-Matter Air Pollution and Its Oxidative Potential in Europe. *Nature* **2020**, *587* (7834), 414−419.

(2) Lelieveld, J.; Pozzer, A.; Pöschl, U.; Fnais, M.; Haines, A.; Münzel, T. Loss of Life Expectancy from Air Pollution Compared to Other Risk Factors: A Worldwide Perspective. *Cardiovasc. Res.* **2020**, *116* (11), 1910−1917.

(3) Stocker, T. F.; Qin, D.; Plattner, G.; Tignor, M. M. B.; Allen, S. K.; Boschung, J.; Nauels, A.; Xia, Y.; Bex, V.; Midgley, P. M. *Climate Change 2013 The Physical Science Basis*; Cambridge University Press: Geneva, 2013https://www.ipcc.ch/site/assets/uploads/2021/08/IPCC_WGI-AR6-Press-Release_en.pdf.

(4) Jimenez, J. L.; Canagaratna, M. R.; Donahue, N. M.; Prevot, A. S. H.; Zhang, Q.; Kroll, J. H.; DeCarlo, P. F.; Allan, J. D.; Coe, H.; Ng, N. L.; Aiken, A. C.; Docherty, K. S.; Ulbrich, I. M.; Grieshop, A. P.; Robinson, A. L.; Duplissy, J.; Smith, J. D.; Wilson, K. R.; Lanz, V. A.; Hueglin, C.; Sun, Y. L.; Tian, J.; Laaksonen, A.; Raatikainen, T.; Rautiainen, J.; Vaattovaara, P.; Ehn, M.; Kulmala, M.; Tomlinson, J. M.; Collins, D. R.; Cubison, M. J.; Dunlea, J. E.; Huffman, J. A.; Onasch, T. B.; Alfarra, M. R.; Williams, P. I.; Bower, K.; Kondo, Y.; Schneider, J.; Drewnick, F.; Borrmann, S.; Weimer, S.; Demerjian, K.; Salcedo, D.; Cottrell, L.; Griffin, R.; Takami, A.; Miyoshi, T.; Hatakeyama, S.; Shimono, A.; Sun, J. Y.; Zhang, Y. M.; Dzepina, K.; Kimmel, J. R.; Sueper, D.; Jayne, J. T.; Herndon, S. C.; Trimborn, A. M.; Williams, L. R.; Wood, E. C.; Middlebrook, A. M.; Kolb, C. E.; Baltensperger, U.; Worsnop, D. R. Evolution of Organic Aerosols in the Atmosphere. *Science* **2009**, *326* (5959), 1525−1529.

(5) Zhang, Q.; Jimenez, J. L.; Canagaratna, M. R.; Allan, J. D.; Coe, H.; Ulbrich, I.; Alfarra, M. R.; Takami, A.; Middlebrook, A. M.; Sun, Y. L.; Dzepina, K.; Dunlea, E.; Docherty, K.; DeCarlo, P. F.; Salcedo, D.; Onasch, T.; Jayne, J. T.; Miyoshi, T.; Shimono, A.; Hatakeyama, S.; Takegawa, N.; Kondo, Y.; Schneider, J.; Drewnick, F.; Borrmann, S.; Weimer, S.; Demerjian, K.; Williams, P.; Bower, K.; Bahreini, R.; Cottrell, L.; Griffin, R. J.; Rautiainen, J.; Sun, J. Y.; Zhang, Y. M.; Worsnop, D. R. Ubiquity and Dominance of Oxygenated Species in Organic Aerosols in Anthropogenically-Influenced Northern Hemisphere Midlatitudes. *Geophys. Res. Lett.* **2007**, *34* (13).

(6) Tang, R.; Lu, Q.; Guo, S.; Wang, H.; Song, K.; Yu, Y.; Tan, R.; Liu, K.; Shen, R.; Chen, S.; Zeng, L.; Jorga, S. D.; Zhang, Z.; Zhang, W.; Shuai, S.; Robinson, A. L. Measurement Report: Distinct Emissions and Volatility Distribution of Intermediate-Volatility Organic Compounds from on-Road Chinese Gasoline Vehicles: Implication of High Secondary Organic Aerosol Formation Potential. *Atmos. Chem. Phys.* **2021**, *21* (4), 2569−2583.

(7) Murphy, D. M.; Cziczo, D. J.; Froyd, K. D.; Hudson, P. K.; Matthew, B. M.; Middlebrook, A. M.; Peltier, R. E.; Sullivan, A.; Thomson, D. S.; Weber, R. J. Single-Particle Mass Spectrometry of Tropospheric Aerosol Particles. *J. Geophys. Res. Atmos.* **2006**, *111* (D23), 23−32.

(8) Kanakidou, M.; Seinfeld, J. H.; Pandis, S. N.; Barnes, I.; Dentener, F. J.; Facchini, M. C.; Van Dingenen, R.; Ervens, B.; Nenes, A.; Nielsen, C. J.; Swietlicki, E.; Putaud, J. P.; Balkanski, Y.; Fuzzi, S.; Horth, J.; Moortgat, G. K.; Winterhalter, R.; Myhre, C. E. L.; Tsigaridis, K.; Vignati, E.; Stephanou, E. G.; Wilson, J. Organic Aerosol and Global Climate Modelling: A Review. *Atmos. Chem. Phys.* **2005**, *5* (4), 1053−1123.

(9) Zhang, Y.; Cai, J.; Wang, S.; He, K.; Zheng, M. Review of Receptor-Based Source Apportionment Research of Fine Particulate Matter and Its Challenges in China. *Sci. Total Environ.* **2017**, *586*, 917−929.

(10) Huang, R.-J.; Zhang, Y.; Bozzetti, C.; Ho, K.-F.; Cao, J.-J.; Han, Y.; Daellenbach, K. R.; Slowik, J. G.; Platt, S. M.; Canonaco, F.; Zotter, P.; Wolf, R.; Pieber, S. M.; Bruns, E. A.; Crippa, M.; Ciarelli, G.; Piazzalunga, A.; Schwikowski, M.; Abbaszade, G.; Schnelle-Kreis, J.; Zimmermann, R.; An, Z.; Szidat, S.; Baltensperger, U.; Haddad, I. E.; Prevot, A. S. H. High Secondary Aerosol Contribution to Particulate Pollution during Haze Events in China. *Nature* **2014**, *514* (7521), 218−222.

(11) Nozière, B.; Kalberer, M.; Claeys, M.; Allan, J.; D'Anna, B.; Decesari, S.; Finessi, E.; Glasius, M.; Grgić, I.; Hamilton, J. F.; Hoffmann, T.; Iinuma, Y.; Jaoui, M.; Kahnt, A.; Kampf, C. J.; Kourtchev, I.; Maenhaut, W.; Marsden, N.; Saarikoski, S.; Schnelle-Kreis, J.; Surratt, J. D.; Szidat, S.; Szmigielski, R.; Wisthaler, A. The Molecular Identification of Organic Compounds in the Atmosphere: State of the Art and Challenges. *Chem. Rev.* **2015**, *115* (10), 3919−3983.

(12) Tao, S.; Lu, X.; Levac, N.; Bateman, A. P.; Nguyen, T. B.; Bones, D. L.; Nizkorodov, S. A.; Laskin, J.; Laskin, A.; Yang, X. Molecular Characterization of Organosulfates in Organic Aerosols from Shanghai and Los Angeles Urban Areas by Nanospray-Desorption Electrospray Ionization High-Resolution Mass Spectrometry. *Environ. Sci. Technol.* **2014**, *48* (18), 10993−11001.

(13) Lin, P.; Rincon, A. G.; Kalberer, M.; Yu, J. Z. Elemental Composition of HULIS in the Pearl River Delta Region, China: Results Inferred from Positive and Negative Electrospray High Resolution Mass Spectrometric Data. *Environ. Sci. Technol.* **2012**, *46* (14), 7454−7462.

(14) Blair, S. L.; MacMillan, A. C.; Drozd, G. T.; Goldstein, A. H.; Chu, R. K.; Paša-Tolić, L.; Shaw, J. B.; Tolić, N.; Lin, P.; Laskin, J.; Laskin, A.; Nizkorodov, S. A. Molecular Characterization of Organosulfur Compounds in Biodiesel and Diesel Fuel Secondary Organic Aerosol. *Environ. Sci. Technol.* **2017**, *51* (1), 119−127.

(15) Vogel, A. L.; Schneider, J.; Müller-Tautges, C.; Phillips, G. J.; Pöhlker, M. L.; Rose, D.; Zuth, C.; Makkonen, U.; Hakola, H.; Crowley, J. N.; Andreae, M. O.; Pöschl, U.; Hoffmann, T. Aerosol Chemistry Resolved by Mass Spectrometry: Linking Field Measurements of Cloud Condensation Nuclei Activity to Organic Aerosol Composition. *Environ. Sci. Technol.* **2016**, *50* (20), 10823−10832.

(16) Vogel, A. L.; Schneider, J.; Müller-Tautges, C.; Klimach, T.; Hoffmann, T. Aerosol Chemistry Resolved by Mass Spectrometry: Insights into Particle Growth after Ambient New Particle Formation. *Environ. Sci. Technol.* **2016**, *50* (20), 10814−10822.

(17) Hoffmann, T.; Huang, R. J.; Kalberer, M. Atmospheric Analytical Chemistry. *Anal. Chem.* **2011**, *83* (12), 4649−4664.

(18) Wang, X.; Hayeck, N.; Brüggemann, M.; Yao, L.; Chen, H.; Zhang, C.; Emmelin, C.; Chen, J.; George, C.; Wang, L. Chemical Characteristics of Organic Aerosols in Shanghai: A Study by Ultrahigh-Performance Liquid Chromatography Coupled With Orbitrap Mass Spectrometry. *J. Geophys. Res. Atmos.* **2017**, *122* (21), 11703−11722.

(19) Wang, K.; Zhang, Y.; Huang, R. J.; Cao, J.; Hoffmann, T. UHPLC-Orbitrap Mass Spectrometric Characterization of Organic Aerosol from a Central European City (Mainz, Germany) and a Chinese Megacity (Beijing). *Atmos. Environ.* **2018**, *189*, 22−29.

(20) Kourtchev, I.; Godoi, R. H. M.; Connors, S.; Levine, J. G.; Archibald, A. T.; Godoi, A. F. L.; Paralovo, S. L.; Barbosa, C. G. G.; Souza, R. A. F.; Manzi, A. O.; Seco, R.; Sjostedt, S.; Park, J.-H.; Guenther, A.; Kim, S.; Smith, J.; Martin, S. T.; Kalberer, M. Molecular Composition of Organic Aerosols in Central Amazonia: An Ultra-High-Resolution Mass Spectrometry Study. *Atmos. Chem. Phys.* **2016**, *16* (18), 11899−11913.

(21) Lin, P.; Yu, J. Z.; Engling, G.; Kalberer, M. Organosulfates in Humic-like Substance Fraction Isolated from Aerosols at Seven Locations in East Asia: A Study by Ultra-High-Resolution Mass Spectrometry. *Environ. Sci. Technol.* **2012**, *46* (24), 13118−13127.

(22) Rincón, A. G.; Calvo, A. I.; Dietzel, M.; Kalberer, M. Seasonal Differences of Urban Organic Aerosol Composition − an Ultra-High Resolution Mass Spectrometry Study. *Environ. Chem.* **2012**, *9* (3), 298.

(23) Huo, Y.; Guo, Z.; Li, Q.; Wu, D.; Ding, X.; Liu, A.; Huang, D.; Qiu, G.; Wu, M.; Zhao, Z.; Sun, H.; Song, W.; Li, X.; Chen, Y.; Wu, T.; Chen, J. Chemical Fingerprinting of HULIS in Particulate Matters Emitted from Residential Coal and Biomass Combustion. *Environ. Sci. Technol.* **2021**, *55* (6), 3593−3603.

https://doi.org/10.1021/acs.est.1c06905
Environ. Sci. Technol. 2022, 56, 7017−7028

(24) Wang, K.; Huang, R. J.; Brüggemann, M.; Zhang, Y.; Yang, L.; Ni, H.; Guo, J.; Wang, M.; Han, J.; Bilde, M.; Glasius, M.; Hoffmann, T. Urban Organic Aerosol Composition in Eastern China Differs from North to South: Molecular Insight from a Liquid Chromatography-Mass Spectrometry (Orbitrap) Study. *Atmos. Chem. Phys.* **2021**, *21* (11), 9089−9104.
(25) Hohrenk, L. L.; Itzel, F.; Baetz, N.; Tuerk, J.; Vosough, M.; Schmidt, T. C. Comparison of Software Tools for Liquid Chromatography−High-Resolution Mass Spectrometry Data Processing in Nontarget Screening of Environmental Samples. *Anal. Chem.* **2020**, *92* (2), 1898−1907.
(26) Vogel, A. L.; Lauer, A.; Fang, L.; Arturi, K.; Bachmeier, F.; Daellenbach, K. R.; Kaser, T.; Vlachou, A.; Pospisilova, V.; Baltensperger, U.; Haddad, I. E.; Schwikowski, M.; Bjelic, S. A Comprehensive Nontarget Analysis for the Molecular Reconstruction of Organic Aerosol Composition from Glacier Ice Cores. *Environ. Sci. Technol.* **2019**, *53* (21), 12565−12575.
(27) Zhao, J.; Qiu, Y.; Zhou, W.; Xu, W.; Wang, J.; Zhang, Y.; Li, L.; Xie, C.; Wang, Q.; Du, W.; Worsnop, D. R.; Canagaratna, M. R.; Zhou, L.; Ge, X.; Fu, P.; Li, J.; Wang, Z.; Donahue, N. M.; Sun, Y. Organic Aerosol Processing During Winter Severe Haze Episodes in Beijing. *J. Geophys. Res. Atmos.* **2019**, *124* (17−18), 10248−10263.
(28) Li, X.; Yang, Y.; Liu, S.; Zhao, Q.; Wang, G.; Wang, Y. Light Absorption Properties of Brown Carbon (BrC) in Autumn and Winter in Beijing: Composition, Formation and Contribution of Nitrated Aromatic Compounds. *Atmos. Environ.* **2020**, *223*, 117289.
(29) Bryant, D. J.; Dixon, W. J.; Hopkins, J. R.; Dunmore, R. E.; Pereira, K. L.; Shaw, M.; Squires, F. A.; Bannan, T. J.; Mehra, A.; Worrall, S. D.; Bacak, A.; Coe, H.; Percival, C. J.; Whalley, L. K.; Heard, D. E.; Slater, E.; Ouyang, B.; Cui, T.; Surratt, J. D.; Liu, D.; Shi, Z.; Harrison, R.; Sun, Y.; Xu, W.; Lewis, A. C.; Lee, J. D.; Rickard, A. R.; Hamilton, J. F. Strong Anthropogenic Control of Secondary Organic Aerosol Formation from Isoprene in Beijing. *Atmos. Chem. Phys.* **2020**, *20* (12), 7531−7552.
(30) Xie, Q.; Su, S.; Chen, S.; Zhang, Q.; Yue, S.; Zhao, W.; Du, H.; Ren, H.; Wei, L.; Cao, D.; Xu, Y.; Sun, Y.; Wang, Z.; Fu, P. Molecular Characterization of Size-Segregated Organic Aerosols in the Urban Boundary Layer in Wintertime Beijing by FT-ICR MS. *Faraday Discuss.* **2021**, *226* (0), 457−478.
(31) Wang, Y.; Hu, M.; Guo, S.; Wang, Y.; Zheng, J.; Yang, Y.; Zhu, W.; Tang, R.; Li, X.; Liu, Y.; Le Breton, M.; Du, Z.; Shang, D.; Wu, Y.; Wu, Z.; Song, Y.; Lou, S.; Hallquist, M.; Yu, J. The Secondary Formation of Organosulfates under Interactions between Biogenic Emissions and Anthropogenic Pollutants in Summer in Beijing. *Atmos. Chem. Phys.* **2018**, *18* (14), 10693−10713.
(32) Du, W.; Dada, L.; Zhao, J.; Chen, X.; Daellenbach, K. R.; Xie, C.; Wang, W.; He, Y.; Cai, J.; Yao, L.; Zhang, Y.; Wang, Q.; Xu, W.; Wang, Y.; Tang, G.; Cheng, X.; Kokkonen, T. V.; Zhou, W.; Yan, C.; Chu, B.; Zha, Q.; Hakala, S.; Kurppa, M.; Järvi, L.; Liu, Y.; Li, Z.; Ge, M.; Fu, P.; Nie, W.; Bianchi, F.; Petäjä, T.; Paasonen, P.; Wang, Z.; Worsnop, D. R.; Kerminen, V.-M.; Kulmala, M.; Sun, Y. A 3D Study on the Amplification of Regional Haze and Particle Growth by Local Emissions. *npj Clim. Atmos. Sci.* **2021**, *4* (1), 1−8.
(33) Steimer, S. S.; Patton, D. J.; Vu, T. V.; Panagi, M.; Monks, P. S.; Harrison, R. M.; Fleming, Z. L.; Shi, Z.; Kalberer, M. Differences in the Composition of Organic Aerosols between Winter and Summer in Beijing: A Study by Direct-Infusion Ultrahigh-Resolution Mass Spectrometry. *Atmos. Chem. Phys.* **2020**, *20* (21), 13303−13318.
(34) Liu, Y.; Yan, C.; Feng, Z.; Zheng, F.; Fan, X.; Zhang, Y.; Li, C.; Zhou, Y.; Lin, Z.; Guo, Y.; Zhang, Y.; Ma, L.; Zhou, W.; Liu, Z.; Dada, L.; Dällenbach, K.; Kontkanen, J.; Cai, R.; Chan, T.; Chu, B.; Du, W.; Yao, L.; Wang, Y.; Cai, J.; Kangasluoma, J.; Kokkonen, T.; Kujansuu, J.; Rusanen, A.; Deng, C.; Fu, Y.; Yin, R.; Li, X.; Lu, Y.; Liu, Y.; Lian, C.; Yang, D.; Wang, W.; Ge, M.; Wang, Y.; Worsnop, D. R.; Junninen, H.; He, H.; Kerminen, V.-M.; Zheng, J.; Wang, L.; Jiang, J.; Petäjä, T.; Bianchi, F.; Kulmala, M. Continuous and Comprehensive Atmospheric Observations in Beijing: A Station to Understand the Complex Urban Atmospheric Environment. *Big Earth Data* **2020**, *4* (3), 295−321.
(35) Cai, J.; Chu, B.; Yao, L.; Yan, C.; Heikkinen, L. M.; Zheng, F.; Li, C.; Fan, X.; Zhang, S.; Yang, D.; Wang, Y.; Kokkonen, T. V.; Chan, T.; Zhou, Y.; Dada, L.; Liu, Y.; He, H.; Paasonen, P.; Kujansuu, J. T.; Petäjä, T.; Mohr, C.; Kangasluoma, J.; Bianchi, F.; Sun, Y.; Croteau, P. L.; Worsnop, D. R.; Kerminen, V. M.; Du, W.; Kulmala, M.; Daellenbach, K. R. Size-Segregated Particle Number and Mass Concentrations from Different Emission Sources in Urban Beijing. *Atmos. Chem. Phys.* **2020**, *20* (21), 12721−12740.
(36) Zhao, Y.; Hallar, A. G.; Mazzoleni, L. R. Atmospheric Organic Matter in Clouds: Exact Masses and Molecular Formula Identification Using Ultrahigh-Resolution FT-ICR Mass Spectrometry. *Atmos. Chem. Phys.* **2013**, *13* (24), 12343−12362.
(37) Yassine, M. M.; Harir, M.; Dabek-Zlotorzynska, E.; Schmitt-Kopplin, P. Structural Characterization of Organic Aerosol Using Fourier Transform Ion Cyclotron Resonance Mass Spectrometry: Aromaticity Equivalent Approach. *Rapid Commun. Mass Spectrom.* **2014**, *28* (22), 2445−2454.
(38) Koch, B. P.; Dittmar, T. From Mass to Structure: An Aromaticity Index for High-Resolution Mass Data of Natural Organic Matter. *Rapid Commun. Mass Spectrom.* **2006**, *20* (5), 926−932.
(39) Daellenbach, K. R.; Kourtchev, I.; Vogel, A. L.; Bruns, E. A.; Jiang, J.; Petäjä, T.; Jaffrezo, J.-L.; Aksoyoglu, S.; Kalberer, M.; Baltensperger, U.; El Haddad, I.; Prévôt, A. S. H. Impact of Anthropogenic and Biogenic Sources on the Seasonal Variation in the Molecular Composition of Urban Organic Aerosols: A Field and Laboratory Study Using Ultra-High-Resolution Mass Spectrometry. *Atmos. Chem. Phys.* **2019**, *19* (9), 5973−5991.
(40) Priestley, M.; Bannan, T. J.; Le Breton, M.; Worrall, S. D.; Kang, S.; Pullinen, I.; Schmitt, S.; Tillmann, R.; Kleist, E.; Zhao, D.; Wildt, J.; Garmash, O.; Mehra, A.; Bacak, A.; Shallcross, D. E.; Kiendler-Scharr, A.; Hallquist, Å. M.; Ehn, M.; Coe, H.; Percival, C. J.; Hallquist, M.; Mentel, T. F.; McFiggans, G. Chemical Characterisation of Benzene Oxidation Products under High- And Low-NOx Conditions Using Chemical Ionisation Mass Spectrometry. *Atmos. Chem. Phys.* **2021**, *21* (5), 3473−3490.
(41) Koss, A. R.; Canagaratna, M. R.; Zaytsev, A.; Krechmer, J. E.; Breitenlechner, M.; Nihill, K. J.; Lim, C. Y.; Rowe, J. C.; Roscioli, J. R.; Keutsch, F. N.; Kroll, J. H. Dimensionality-Reduction Techniques for Complex Mass Spectrometric Datasets: Application to Laboratory Atmospheric Organic Oxidation Experiments. *Atmos. Chem. Phys.* **2020**, *20* (2), 1021−1041.
(42) Slater, J.; Tonttila, J.; McFiggans, G.; Coe, H.; Romakkaniemi, S.; Sun, Y.; Xu, W.; Fu, P.; Wang, Z. Using a Coupled LES Aerosol−Radiation Model to Investigate the Importance of Aerosol−Boundary Layer Feedback in a Beijing Haze Episode. *Faraday Discuss.* **2021**, *226* (0), 173−190.
(43) Fleming, L. T.; Ali, N. N.; Blair, S. L.; Roveretto, M.; George, C.; Nizkorodov, S. A. Formation of Light-Absorbing Organosulfates during Evaporation of Secondary Organic Material Extracts in the Presence of Sulfuric Acid. *ACS Earth Sp. Chem.* **2019**, *3* (6), 947−957.
(44) Estillore, A. D.; Hettiyadura, A. P. S.; Qin, Z.; Leckrone, E.; Wombacher, B.; Humphry, T.; Stone, E. A.; Grassian, V. H. Water Uptake and Hygroscopic Growth of Organosulfate Aerosol. *Environ. Sci. Technol.* **2016**, *50* (8), 4259−4268.
(45) Peng, C.; Razafindrambinina, P. N.; Malek, K. A.; Chen, L.; Wang, W.; Huang, R. J.; Zhang, Y.; DIng, X.; Ge, M.; Wang, X.; Asa-Awuku, A. A.; Tang, M. Interactions of Organosulfates with Water Vapor under Sub- And Supersaturated Conditions. *Atmos. Chem. Phys.* **2021**, *21* (9), 7135−7148.
(46) Brüggemann, M.; Xu, R.; Tilgner, A.; Kwong, K. C.; Mutzel, A.; Poon, H. Y.; Otto, T.; Schaefer, T.; Poulain, L.; Chan, M. N.; Herrmann, H. Organosulfates in Ambient Aerosol: State of Knowledge and Future Research Directions on Formation, Abundance, Fate, and Importance. *Environ. Sci. Technol.* **2020**, *54* (7), 3767−3782.
(47) Lu, C.; Wang, X.; Li, R.; Gu, R.; Zhang, Y.; Li, W.; Gao, R.; Chen, B.; Xue, L.; Wang, W. Emissions of Fine Particulate Nitrated Phenols from Residential Coal Combustion in China. *Atmos. Environ.* **2019**, *203*, 10−17.

https://doi.org/10.1021/acs.est.1c06905
Environ. Sci. Technol. 2022, 56, 7017−7028

(48) Olson, M. R.; Victoria Garcia, M.; Robinson, M. A.; Van Rooy, P.; Dietenberger, M. A.; Bergin, M.; Schauer, J. J. Investigation of Black and Brown Carbon Multiple-Wavelength-Dependent Light Absorption from Biomass and Fossil Fuel Combustion Source Emissions. *J. Geophys. Res. Atmos.* **2015**, *120* (13), 6682−6697.
(49) Lin, P.; Fleming, L. T.; Nizkorodov, S. A.; Laskin, J.; Laskin, A. Comprehensive Molecular Characterization of Atmospheric Brown Carbon by High Resolution Mass Spectrometry with Electrospray and Atmospheric Pressure Photoionization. *Anal. Chem.* **2018**, *90* (21), 12493−12502.
(50) Wang, X.; Gu, R.; Wang, L.; Xu, W.; Zhang, Y.; Chen, B.; Li, W.; Xue, L.; Chen, J.; Wang, W. Emissions of Fine Particulate Nitrated Phenols from the Burning of Five Common Types of Biomass. *Environ. Pollut.* **2017**, *230*, 405−412.
(51) Teich, M.; Van Pinxteren, D.; Wang, M.; Kecorius, S.; Wang, Z.; Müller, T.; Močnik, G.; Herrmann, H. Contributions of Nitrated Aromatic Compounds to the Light Absorption of Water-Soluble and Particulate Brown Carbon in Different Atmospheric Environments in Germany and China. *Atmos. Chem. Phys.* **2017**, *17* (3), 1653−1672.
(52) Taneda, S.; Mori, Y.; Kamata, K.; Hayashi, H.; Furuta, C.; Li, C.; Seki, K. I.; Sakushima, A.; Yoshino, S.; Yamaki, K.; Watanabe, G.; Taya, K.; Suzuki, A. K. Estrogenic and Anti-Androgenic Activity of Nitrophenols in Diesel Exhaust Particles (DEP). *Biol. Pharm. Bull.* **2004**, *27* (6), 835−837.
(53) Inomata, S.; Tanimoto, H.; Fujitani, Y.; Sekimoto, K.; Sato, K.; Fushimi, A.; Yamada, H.; Hori, S.; Kumazawa, Y.; Shimono, A.; Hikida, T. On-Line Measurements of Gaseous Nitro-Organic Compounds in Diesel Vehicle Exhaust by Proton-Transfer-Reaction Mass Spectrometry. *Atmos. Environ.* **2013**, *73*, 195−203.
(54) Perrone, M. G.; Carbone, C.; Faedo, D.; Ferrero, L.; Maggioni, A.; Sangiorgi, G.; Bolzacchini, E. Exhaust Emissions of Polycyclic Aromatic Hydrocarbons, n-Alkanes and Phenols from Vehicles Coming within Different European Classes. *Atmos. Environ.* **2014**, *82*, 391−400.
(55) Lu, C.; Wang, X.; Dong, S.; Zhang, J.; Li, J.; Zhao, Y.; Liang, Y.; Xue, L.; Xie, H.; Zhang, Q.; Wang, W. Emissions of Fine Particulate Nitrated Phenols from Various On-Road Vehicles in China. *Environ. Res.* **2019**, *179*.
(56) Yuan, W.; Huang, R. J.; Yang, L.; Wang, T.; Duan, J.; Guo, J.; Ni, H.; Chen, Y.; Chen, Q.; Li, Y.; Dusek, U.; O'Dowd, C.; Hoffmann, T. Measurement Report: PM2.5-Bound Nitrated Aromatic Compounds in Xi'an, Northwest China - Seasonal Variations and Contributions to Optical Properties of Brown Carbon. *Atmos. Chem. Phys.* **2021**, *21* (5), 3685−3697.
(57) Kitanovski, Z.; Grgić, I.; Vermeylen, R.; Claeys, M.; Maenhaut, W. Liquid Chromatography Tandem Mass Spectrometry Method for Characterization of Monoaromatic Nitro-Compounds in Atmospheric Particulate Matter. *J. Chromatogr. A* **2012**, *1268*, 35−43.
(58) Mohr, C.; Lopez-Hilfiker, F. D.; Zotter, P.; Prevot, A. S. H.; Xu, L.; Ng, N. L.; Herndon, S. C.; Williams, L. R.; Franklin, J. P.; Zahniser, M. S.; Worsnop, D. R.; Knighton, W. B.; Aiken, A. C.; Gorkowski, K. J.; Dubey, M. K.; Allan, J. D.; Thornton, J. A. Contribution of Nitrated Phenols to Wood Burning Brown Carbon Light Absorption in Detling, United Kingdom during Winter Time. *Environ. Sci. Technol.* **2013**, *47* (12), 6316−6324.
(59) Kautzman, K. E.; Surratt, J. D.; Chan, M. N.; Chan, A. W. H.; Hersey, S. P.; Chhabra, P. S.; Dalleska, N. F.; Wennberg, P. O.; Flagan, R. C.; Seinfeld, J. H. Chemical Composition of Gas- and Aerosol-Phase Products from the Photooxidation of Naphthalene. *J. Phys. Chem. A* **2010**, *114* (2), 913−934.
(60) Wang, K.; Huang, R.-J. J.; Brüggemann, M.; Zhang, Y.; Yang, L.; Ni, H.; Guo, J.; Wang, M.; Han, J.; Bilde, M.; Glasius, M.; Hoffmann, T. Urban Organic Aerosol Composition in Eastern China Differs from North to South: Molecular Insight from a Liquid Chromatography-Orbitrap Mass Spectrometry Study. *Atmos. Chem. Phys.* **2021**, *21* (11), 9089−9104.
(61) Tuhkanen Tuula, A.; Beltrán Fernando, J. Intermediates of the Oxidation of Naphthalene in Water with the Combination of Hydrogen Peroxide and UV Radiation. *Chemosphere* **1995**, *30* (8), 1463−1475.
(62) He, X.; Huang, X. H. H.; Chow, K. S.; Wang, Q.; Zhang, T.; Wu, D.; Yu, J. Z. Abundance and Sources of Phthalic Acids, Benzene-Tricarboxylic Acids, and Phenolic Acids in PM2.5 at Urban and Suburban Sites in Southern China. *ACS Earth Sp. Chem.* **2018**, *2* (2), 147−158.
(63) Fraser, M. P.; Cass, G. R.; Simoneit, B. R. T. Gas-Phase and Particle-Phase Organic Compounds Emitted from Motor Vehicle Traffic in a Los Angeles Roadway Tunnel. *Environ. Sci. Technol.* **1998**, *32* (14), 2051−2060.
(64) Li, M.; McDow, S. R.; Tollerud, D. J.; Mazurek, M. A. Seasonal Abundance of Organic Molecular Markers in Urban Particulate Matter from Philadelphia, PA. *Atmos. Environ.* **2006**, *40* (13), 2260−2273.
(65) Duan, X.; Li, Y. Sources and Fates of BTEX in the General Environment and Its Distribution in Coastal Cities of China. *J. Environ. Sci. Public Heal.* **2017**, *1* (2), 86−106.
(66) Jüttner, F. Emission of Aromatic Hydrocarbons and Aldehydes into the Water by a Four-Stroke Outboard Motor: Quantitative Measurements. *Chemosphere* **1994**, *29* (2), 191−200.
(67) Wu, T. G.; Chang, J. C.; Huang, S. H.; Lin, W. Y.; Chan, C. C.; Wu, C. F. Exposures and Health Impact for Bicycle and Electric Scooter Commuters in Taipei. *Transp. Res. Part D Transp. Environ.* **2021**, *91*, 102696.
(68) Hsieh, P. Y.; Shearston, J. A.; Hilpert, M. Benzene Emissions from Gas Station Clusters: A New Framework for Estimating Lifetime Cancer Risk. *J. Environ. Heal. Sci. Eng.* **2021**, *19* (1), 273−283.
(69) Varjani, S. J.; Gnansounou, E.; Pandey, A. Comprehensive Review on Toxicity of Persistent Organic Pollutants from Petroleum Refinery Waste and Their Degradation by Microorganisms. *Chemosphere* **2017**, *188*, 280−291.
(70) Wang, X. K.; Rossignol, S.; Ma, Y.; Yao, L.; Wang, M. Y.; Chen, J. M.; George, C.; Wang, L. Molecular Characterization of Atmospheric Particulate Organosulfates in Three Megacities at the Middle and Lower Reaches of the Yangtze River. *Atmos. Chem. Phys.* **2016**, *16* (4), 2285−2298.
(71) Surratt, J. D.; Gómez-González, Y.; Chan, A. W. H.; Vermeylen, R.; Shahgholi, M.; Kleindienst, T. E.; Edney, E. O.; Offenberg, J. H.; Lewandowski, M.; Jaoui, M.; Maenhaut, W.; Claeys, M.; Flagan, R. C.; Seinfeld, J. H. Organosulfate Formation in Biogenic Secondary Organic Aerosol. *J. Phys. Chem. A* **2008**, *112* (36), 8345−8378.
(72) Hettiyadura, A. P. S.; Stone, E. A.; Kundu, S.; Baker, Z.; Geddes, E.; Richards, K.; Humphry, T. Determination of Atmospheric Organosulfates Using HILIC Chromatography with MS Detection. *Atmos. Meas. Technol.* **2015**, *8* (6), 2347−2358.
(73) Barbosa, T. S.; Riva, M.; Chen, Y.; da Silva, C. M.; Ameida, J. C. S.; Zhang, Z.; Gold, A.; Arbilla, G.; Bauerfeldt, G. F.; Surratt, J. D. Chemical Characterization of Organosulfates from the Hydroxyl Radical-Initiated Oxidation and Ozonolysis of Cis-3-Hexen-1-Ol. *Atmos. Environ.* **2017**, *162*, 141−151.
(74) Wang, K.; Zhang, Y.; Huang, R. J.; Wang, M.; Ni, H.; Kampf, C. J.; Cheng, Y.; Bilde, M.; Glasius, M.; Hoffmann, T. Molecular Characterization and Source Identification of Atmospheric Particulate Organosulfates Using Ultrahigh Resolution Mass Spectrometry. *Environ. Sci. Technol.* **2019**, *53* (11), 6192−6202.
(75) Gómez-González, Y.; Surratt, J. D.; Cuyckens, F.; Szmigielski, R.; Vermeylen, R.; Jaoui, M.; Lewandowski, M.; Offenberg, J. H.; Kleindienst, T. E.; Edney, E. O.; Blockhuys, F.; Van Alsenoy, C.; Maenhaut, W.; Claeys, M. Characterization of Organosulfates from the Photooxidation of Isoprene and Unsaturated Fatty Acids in Ambient Aerosol Using Liquid Chromatography/(−) Electrospray Ionization Mass Spectrometry. *J. Mass Spectrom.* **2008**, *43* (3), 371−382.
(76) Glasius, M.; Hansen, A. M. K.; Claeys, M.; Henzing, J. S.; Jedynska, A. D.; Kasper-Giebl, A.; Kistler, M.; Kristensen, K.; Martinsson, J.; Maenhaut, W.; Nøjgaard, J. K.; Spindler, G.; Stenström, K. E.; Swietlicki, E.; Szidat, S.; Simpson, D.; Yttri, K. E.

https://doi.org/10.1021/acs.est.1c06905
Environ. Sci. Technol. 2022, 56, 7017−7028

Composition and Sources of Carbonaceous Aerosols in Northern Europe during Winter. *Atmos. Environ.* **2018**, *173*, 127−141.
(77) Zhang, Y.; Wang, K.; Tong, H.; Huang, R.; Hoffmann, T. The Maximum Carbonyl Ratio (MCR) as a New Index for the Structural Classification of Secondary Organic Aerosol Components. *Rapid Commun. Mass Spectrom.* **2021**, *35*, e9113.
(78) Müller, L.; Reinnig, M.-C.; Naumann, K. H.; Saathoff, H.; Mentel, T. F.; Donahue, N. M.; Hoffmann, T. Formation of 3-Methyl-1,2,3-Butanetricarboxylic Acid via Gas Phase Oxidation of Pinonic Acid − a Mass Spectrometric Study of SOA Aging. *Atmos. Chem. Phys.* **2012**, *12* (3), 1483−1496.
(79) Christoffersen, T. S.; Hjorth, J.; Horie, O.; Jensen, N. R.; Kotzias, D.; Molander, L. L.; Neeb, P.; Ruppert, L.; Winterhalter, R.; Virkkula, A.; Wirtz, K.; Larsen, B. R. Cis-Pinic Acid, a Possible Precursor for Organic Aerosol Formation from Ozonolysis of α-Pinene. *Atmos. Environ.* **1998**, *32* (10), 1657−1661.
(80) Jenkin, M. E.; Shallcross, D. E; Harvey, J. N Development and Application of a Possible Mechanism for the Generation of Cis-Pinic Acid from the Ozonolysis of α- and β-Pinene. *Atmos. Environ.* **2000**, *34* (18), 2837−2850.
(81) Koch, S.; Winterhalter, R.; Uherek, E.; Kolloff, A.; Neeb, P.; Moortgat, G. K. Formation of New Particles in the Gas-Phase Ozonolysis of Monoterpenes. *Atmos. Environ.* **2000**, *34* (23), 4031−4042.
(82) Kroll, J. H.; Donahue, N. M.; Jimenez, J. L.; Kessler, S. H.; Canagaratna, M. R.; Wilson, K. R.; Altieri, K. E.; Mazzoleni, L. R.; Wozniak, A. S.; Bluhm, H.; Mysak, E. R.; Smith, J. D.; Kolb, C. E.; Worsnop, D. R. Carbon Oxidation State as a Metric for Describing the Chemistry of Atmospheric Organic Aerosol. *Nat. Chem.* **2011**, *3* (2), 133−139.
(83) Brüggemann, M.; van Pinxteren, D.; Wang, Y.; Yu, J. Z.; Herrmann, H. Quantification of Known and Unknown Terpenoid Organosulfates in PM10 Using Untargeted LC−HRMS/MS: Contrasting Summertime Rural Germany and the North China Plain. *Environ. Chem.* **2019**, *16* (5), 333.
(84) Wang, Y.; Ren, J.; Huang, X. H. H.; Tong, R.; Yu, J. Z. Synthesis of Four Monoterpene-Derived Organosulfates and Their Quantification in Atmospheric Aerosol Samples. *Environ. Sci. Technol.* **2017**, *51* (12), 6791−6801.
(85) Kristensen, K.; Glasius, M. Organosulfates and Oxidation Products from Biogenic Hydrocarbons in Fine Aerosols from a Forest in North West Europe during Spring. *Atmos. Environ.* **2011**, *45* (27), 4546−4556.
(86) Bryant, D. J.; Elzein, A.; Newland, M.; White, E.; Swift, S.; Watkins, A.; Deng, W.; Song, W.; Wang, S.; Zhang, Y.; Wang, X.; Rickard, A. R.; Hamilton, J. F. Importance of Oxidants and Temperature in the Formation of Biogenic Organosulfates and Nitrooxy Organosulfates. *ACS Earth Sp. Chem.* **2021**, *5* (9), 2291−2306.
(87) Brüggemann, M.; Riva, M.; Perrier, S.; Poulain, L.; George, C.; Herrmann, H. Overestimation of Monoterpene Organosulfate Abundance in Aerosol Particles by Sampling in the Presence of SO2. *Environ. Sci. Technol. Lett.* **2021**, *8* (3), 206−211.
(88) Kourtchev, I.; Doussin, J. F.; Giorio, C.; Mahon, B.; Wilson, E. M.; Maurin, N.; Pangui, E.; Venables, D. S.; Wenger, J. C.; Kalberer, M. Molecular Composition of Fresh and Aged Secondary Organic Aerosol from a Mixture of Biogenic Volatile Compounds: A High-Resolution Mass Spectrometry Study. *Atmos. Chem. Phys.* **2015**, *15* (10), 5683−5695.

https://doi.org/10.1021/acs.est.1c06905
Environ. Sci. Technol. 2022, 56, 7017−7028